November 2, 2009

Study of isolation properties of SUSY low-p_T leptons.

Z. Hatherell[a)], G. Karapostoli[a)], M. Pioppi[a,b)],
A. Savin[c)], A. Sparrow[a)], M. Weinberg[c)]

a) Imperial College London, United Kingdom

b) INFN e Dipartimento di Fisica, Perugia, Italy

c) University of Wisconsin, Madison, United States

Abstract

Events with leptons in the final state will play a significant role in SUSY searches at initial LHC luminosities. The energy spectra of the leptons is expected to be soft, especially in models where the mass difference between the initial SUSY particle and the lightest SUSY particle (LSP) is small. Optimization of isolation cuts for electrons in the transverse momentum range $5 < p_T < 30$ GeV and for muons in the range $3 < p_T < 30$ GeV is discussed. The results are presented in terms of SUSY lepton reconstruction efficiency and rejection of fake leptons and leptons from heavy quark decays. Lepton selections for single- and double-lepton SUSY final states are proposed.

1 Introduction

Events with leptons in the final state will play a significant role in SUSY searches already at initial LHC luminosities. They complement the fully-hadronic searches, providing cleaner signatures than those based just on jets and missing energy.

SUSY models predict significant lepton production from decay of sparticles. The primary sources of leptons are expected to be:

$$\tilde{\chi}_2^0 \to l^{\pm} + \tilde{l}^{\mp}$$
$$\tilde{\chi}_1^{\pm} \to l^{\pm} + \tilde{\nu}_l$$
$$\tilde{l}^{\pm} \to l^{\pm} + \tilde{\chi}_1^0$$

The p_T spectrum of the resulting leptons depends strongly on the mass difference between the initial and final SUSY particles. For the cases in which the two SUSY particles are more nearly mass-degenerate, the lepton p_T spectrum is expected to be soft, and therefore a high lepton-reconstruction efficiency and background rejection at low transverse momentum is required.

The standard lepton-isolation recommendations at CMS proposed by the V + Jets Cross-PAG [1] have been shown to work well for lepton-p_T above ~ 30 GeV/c. For lower-p_T leptons, however, these cuts can have a much more pronounced impact on the efficiency. For this reason, it is natural to look at separate optimization of the isolation requirements for soft leptons.

2 Lepton reconstruction and isolation requirements

The analysis was performed within the SUSY PAT framework [2]. From the PAT data format, reduced ntuples were produced using the procedure described elsewhere [3]. The data samples are summarized in Table 1.

Sample	N MC events	σ (pb)
SUSY (LM1)	104800	16.06
QCD (Pythia)	27267325	1.568 $\times 10^9$

Table 1: MC samples used for the isolation study.

For the purposes of the lepton isolation performace study, we have developed a lepton classification tool based on the Monte Carlo (MC) truth information. Reconstructed electrons and muons are matched to generator level leptons (e or μ's), and split into the following categories, according to the MC mother of the generated particle: i) "Prompt" leptons, are identified as the ones originated by the decay of a SUSY particle, a W/Z or a τ. ii) "Heavy-flavor" leptons, are coming from the hadronic decays of heavy-flavor quarks (b/c decays). iii) "Fake" leptons are typically identified as reconstructed leptons faked by a jet. In the case of muons, the latter category includes in-flight decays of π/K-mesons, as well as jet punch-through.

Matching between generated and reconstructed leptons was performed using a cone in (η, ϕ) phase space. The distance between generated and reconstructed leptons, $\Delta R = \sqrt{(\Delta\eta)^2 + (\Delta\phi)^2}$, was required to be less then 0.5, and the closest generated lepton was associated with the corresponding reconstructed candidate. If no generated lepton was found within the ΔR cone the reconstructed lepton was considered to be a "fake".

The leptons were reconstructed at detector level and passed identification procedure [4, 5]. Electrons that satisfied RobustLoose and muons that satisfied GlobalTight identification requirements were selected. Generated and reconstructed electrons were required to have $p_T > 5$ GeV and $|\eta| < 2.5$, muons, $p_T > 3$ GeV and $|\eta| < 2.1$. In order to reduce contribution form the HF and fake leptons, additional requirements on the lepton qualiity were applied:

- Transverse impact parameter corrected for the beam spot < 2 mm
- Normalized global $\chi^2 < 10$ (only for muons)
- Number of hits in the tracker track > 11 (only for muons)

Lepton reconstruction efficiency, defined as a ratio of the number of reconstructed and matched leptons to the total number of generated leptons, was estimated using prompt leptons from the SUSY LM1 sample. The efficiency is presented in Fig. 1 for (a) electrons and (b) muons as a function of generated lepton p_T. The efficiency decreases with decreasing lepton p_T, and corresponds to $\sim 60\%$ in the lowest p_T bins considered in this analysis.

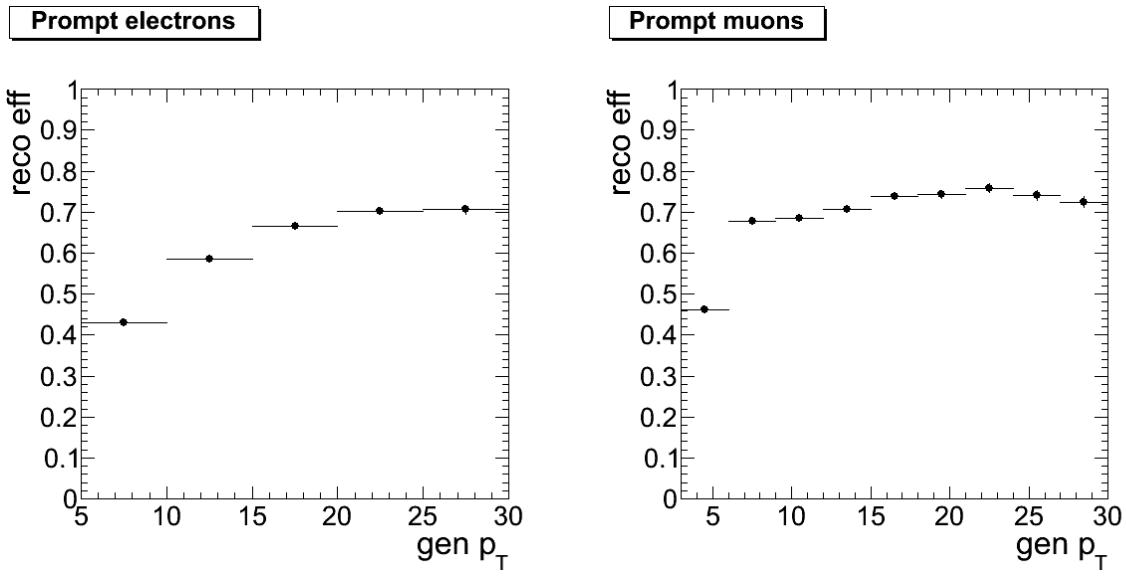

Figure 1: Reconstruction efficiency for (a) prompt electrons and (b) prompt muons as a function of generated lepton p_T.

Isolation properties of the reconstructed leptons were studied using following isolation variables:

$$\begin{aligned}
\text{iso}_{\text{abs}}^{\text{track}} &= \sum_{\Delta R<0.3} p_T^{\text{track}} \\
\text{iso}_{\text{abs}}^{\text{ECAL}} &= \sum_{\Delta R<0.3} E_T^{\text{ECAL}} \\
\text{iso}_{\text{abs}}^{\text{HCAL}} &= \sum_{\Delta R<0.3} E_T^{\text{HCAL}} \\
\text{iso}_{\text{abs}}^{\text{comb}} &= \sum_{\Delta R<0.3} \left(p_T^{\text{track}} + E_T^{\text{ECAL+HCAL}}\right)
\end{aligned}$$

where $\sum_{\Delta R<0.3} p_T^{\text{track}}$ is the sum of the transverse momenta of the tracks in a cone ($\Delta R < 0.3$) around the lepton direction. $\sum_{\Delta R<0.3} E_T^{\text{ECAL}}$ and $\sum_{\Delta R<0.3} E_T^{\text{HCAL}}$ are the sums of the transverse energy measured in a cone ($\Delta R < 0.3$) around the lepton direction in the electromagnetic and hadronic calorimeter respectively. Relative isolation was defined as a ratio of the absolute isolation to reconstructed transverse momentum, p_T, of the examined lepton.

A scatter plot of combined relative isolation as a function of reconstructed lepton p_T is presented in Fig. 2 for prompt, HF and fake leptons respectively. The V + Jets Cross-PAG recommended cut of 0.1 is also shown. At low p_T values the cut rejects a significant fraction of signal events; therefore, additional optimization of the isolation procedure is needed. Since the isolation depends on the lepton transverse momentum, the optimization is done in multiple bins of lepton p_T. Five bins of 5 GeV width: 5 – 10 GeV, 10 – 15 GeV, ..., 25 – 30 GeV for electrons and nine bins of 3 GeV width: 3 – 6 GeV, 6 – 9 GeV, ..., 27 – 30 GeV for muons. The lower limits on the p_T ranges represent the softest leptons that can be reconstructed within the PAT framework and bin width is choosen based on energy resolution.

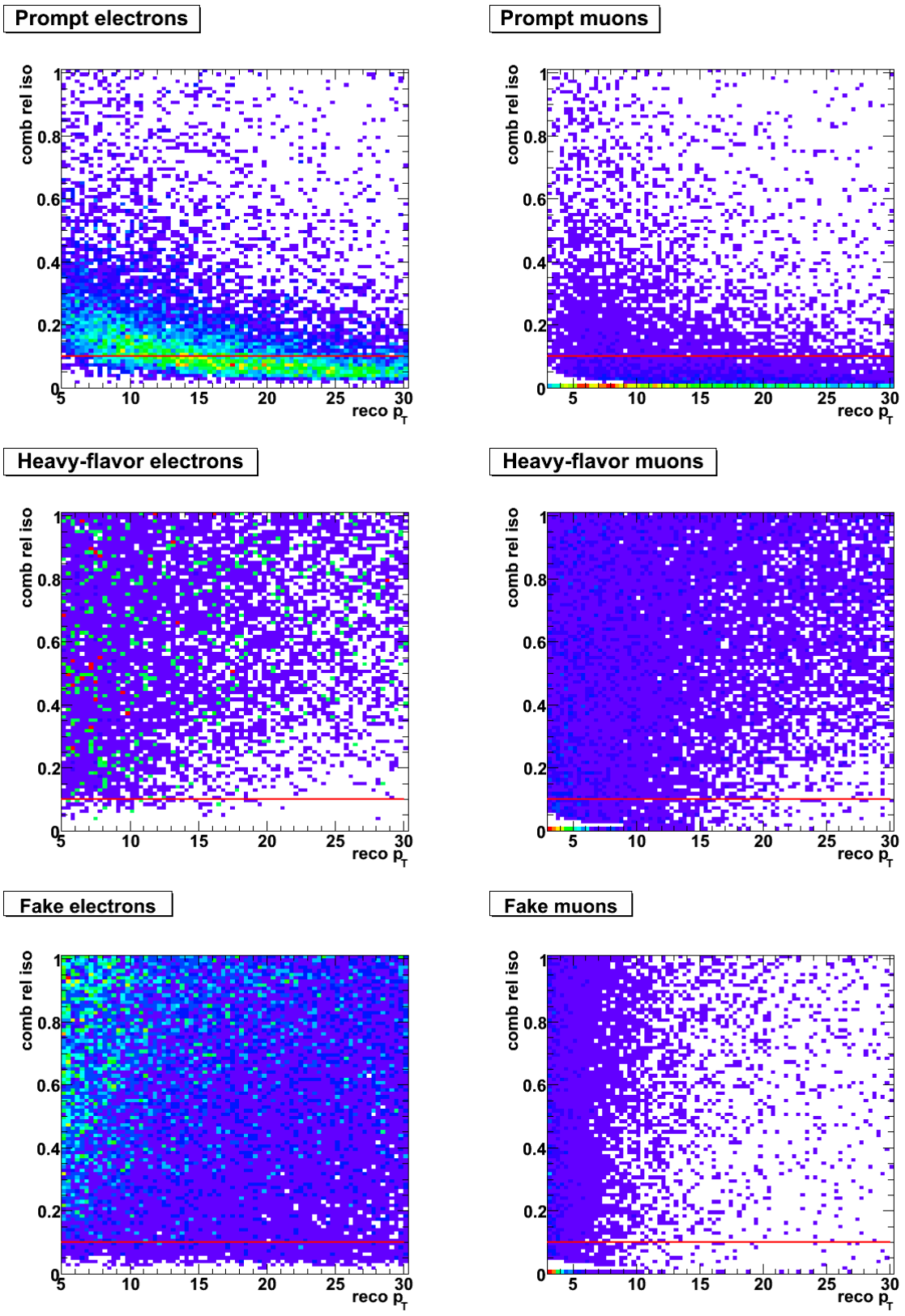

Figure 2: Combined relative isolation as a function of reconstructed p_T for prompt (top), HF (middle) and fake (bottom) leptons. Electrons are shown on the left while muons are on the right.

3 Optimization of isolation requirements for low-p_T leptons

The optimization of the isolation for leptons originating from SUSY processes requires an additional cut $HT > 300\text{GeV}$, where $HT = \left(\sum_{\text{jets}} p_T + \sum_{\text{lep}} p_T\right)$, and the sums run over all the reconstructed leptons and all the reconstructed hadronic jets with a tranverse energy greater than 50 GeV. This cut defines an energy scale which is expected in SUSY production.

The optimization procedure was based on a comparison of signal efficiency and background rejection. Efficiency as a function of isolation cut, eff(x), was defined as the ratio of reconstructed leptons with isolation $< x$ to all reconstructed leptons. Rejection as a function of isolation cut, rej(x), was defined as the ratio of reconstructed leptons with isolation $> x$ to all reconstructed leptons, i.e. for all cut values x, rej$(x) = 1 - \text{eff}(x)$. Figure 3 shows prompt lepton efficiency as a function of background lepton rejection for each isolation variable.

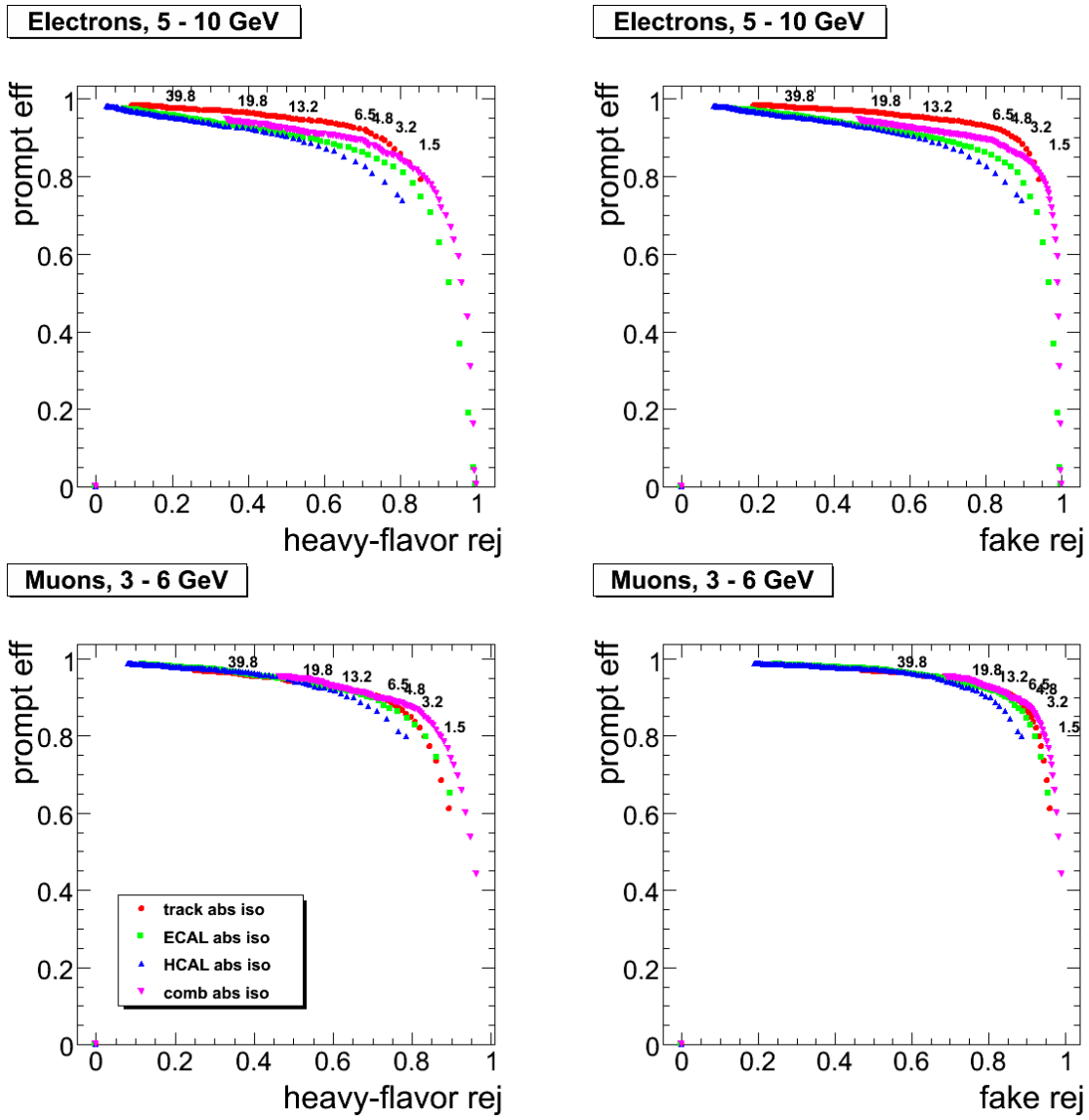

Figure 3: Prompt leptons efficiency with respect to background rejection for HF (left) and fake leptons (right) in p_T region from 5 to 10 GeV for electrons (top) and in p_T region from 3 to 6 GeV for muons (bottom). Each point on the graph represents a different cut on absolute isolation calculated from the tracker (first curve), the ECAL (second curve) or the HCAL (third curve).

For both electrons and muons, tracker isolation demonstrates greater discriminating power than ECAL or HCAL isolation. Additionally in the LHC startup scenario, the low p_T tracks (which mainly contribute to the soft lepton isolation) are expected to be more reliable than the low p_T energy deposits in the calorimeters, therefore only the tracker isolation is considered in the first step of the optimization.

Since signal to background conditions differ depending on SUSY analysis four optimization approaches were considered:

- **PureHF**
  Highest cut on isolation at which $\text{rej}_{\text{HF}} \geq 0.9$
- **PureFake**
  Highest cut on isolation at which $\text{rej}_{\text{fake}} \geq 0.9$
- **Optimal**
  Minimizes $x = \sqrt{(1-\text{eff})^2 + (1-\text{rej})^2}$
- **Efficient**
  Lowest cut on isolation at which $\text{eff}_{\text{prompt}} \geq 0.9$

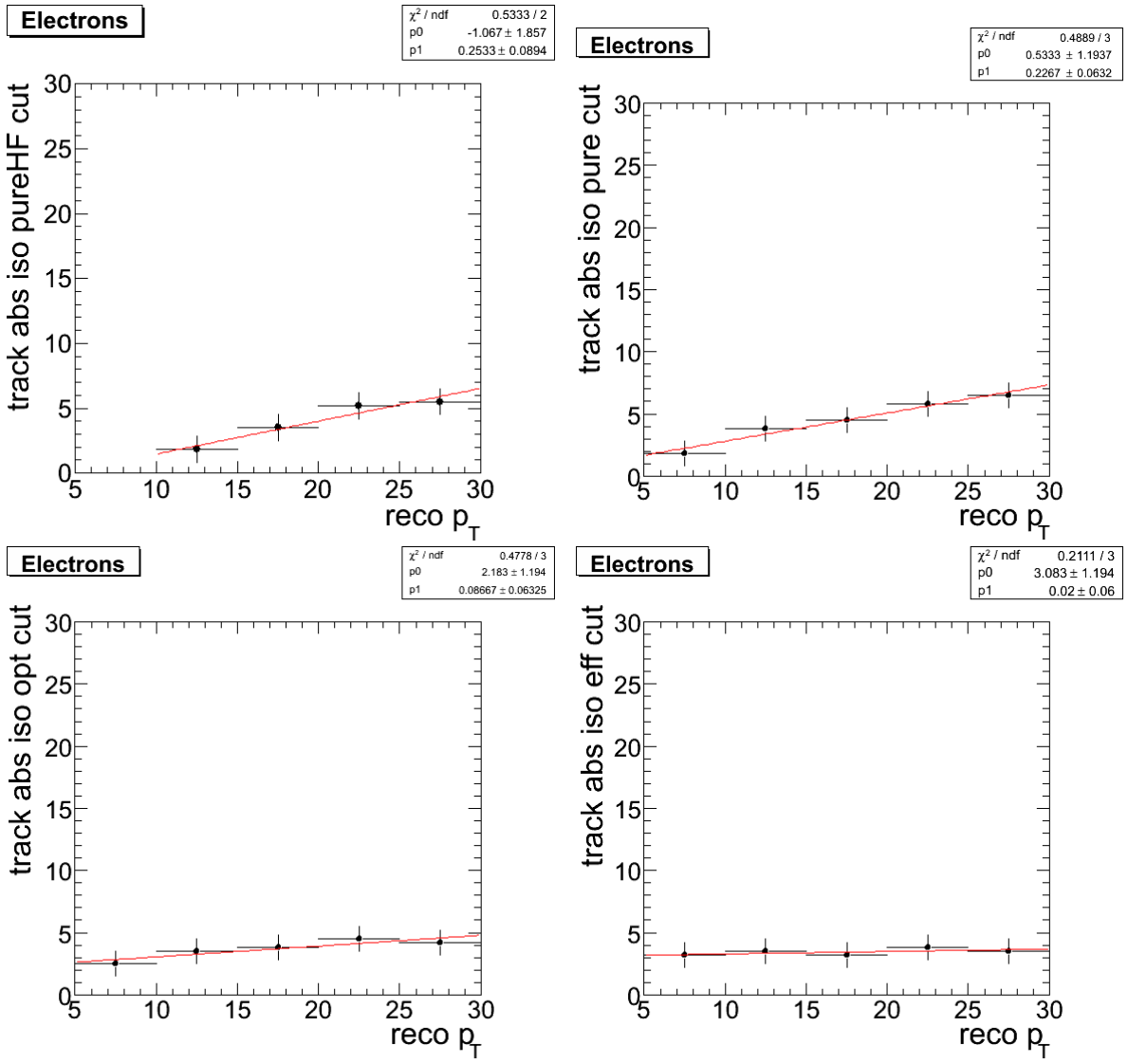

Figure 4: Tracker isolation cut values for electrons as a function of p_T for **pureHF**(top left), **pureFake** (top right), **optimal** (bottom left) and **efficient** (bottom right) optimization procedure.

Figure 4 shows the optimized cut values as a function of the electron transverse momentum. Linear fits to the data are also shown. The lowest-p_T bin for the **pureHF** procedure is empty, since the required 0.9 rejection power can not be achieved by using tracking information only. The **pure** procedures demonstrate an increase of the isolation cat with p_T increase, the **efficient** requirement allows the isolation cut to be almost constant with p_T.

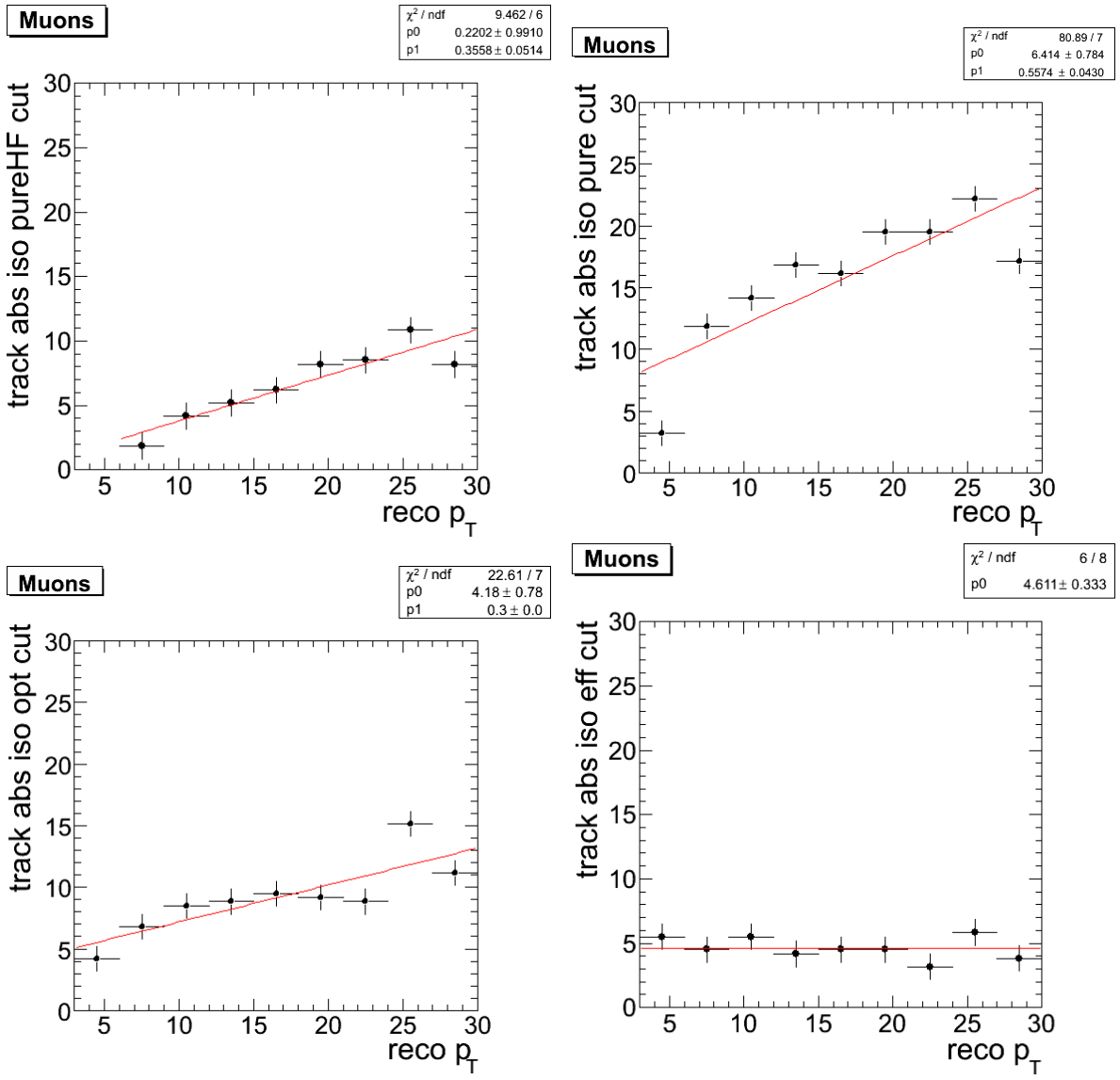

Figure 5: Tracker isolation cut values for muons as a function of p_T for **pureHF** (top left), **pureFake** (top right), **optimal** (bottom left), **efficient** (bottom right) optimization procedure.

The optimization results for muons are presented in Fig. 5. The results demonstrate behaviour similar to those for muons but in general the cuts are less stringent.

The results of the optimization procedure are summarized in App. A and App. B.

4 Optimization of ECAL isolation after applying cuts on tracker isolation

An additonal background rejection power of the isolation procedure can be achieved by applying the ECAL isolation after the tracking isolation was applied. The **efficient** tracking procedure as shown in Figs. 4 and 5 was chosen. For simplicity the tracking isolation was set to 3 GeV for electrons and 5 GeV for muons.

Prompt lepton efficiency with respect to the background lepton rejection is shown in Fig. 6 for different cuts on ECAL isolation for leptons in the lowest p_T bin. The complete set of plots for each p_T bin is given in App. C. It is demonstrated that by using the ECAL isolation after tracking isolation any background rejection power can be achieved for electrons but efficiency of the prompt electrons drop significantly as rejection power increases. For muons it is not the case and there is a limit on rejection power which can not be exceeded. The dependence of the prompt muons efficiency on the isolation is much weaker than those observed for electrons.

5 Low-P_T Isolation for SUSY analysis

The results of isolation studies described in Sec. 3 were applied to Single Lepton (SL) and Same Sign Dilepton (SSD) SUSY analyses. For SL analysis, which is strongly affected by a high fake lepton rate, both the **pure** and the **optimal** cuts have been applied for comparison. The **pureFake** is applied to electrons, while the **pureHF** is applied to muons, as in the muon channel the background from heavy-flavour decays is expected to be higher than that from fakes. For SSDL analysis, for which the request of two same-sign leptons significantly increases the background rejection, the **efficient** cuts definition was used. In both cases the results after applying the V+jets cuts are also shown for comparison.

5.1 Single Lepton analysis

The SL analysis comprise a general-purpose search for supersymmetry in events containing one-electron or one-muon in the final state, in addition to multiple jets and large missing transverse energy.

The CMS SUSY group provides a set of baseline selection criteria for the single lepton analysis in the context of the Single-lepton Reference Analysis 4 (RA4) [6]. For what concerns the electron and muon isolation requirements, the RA4 suggests the standard V+jets recommendations. A comparison between the recommended V+jets isolation and the proposed Soft Lepton (SL) isolation selection is presented in terms of performance of the signal-to-background ratio and signal significance. The trigger requirement of RA4 in the one-electron channel is deliberately ommitted, to allow the investigation of lowering the electron offline momentum threshold down to 5 GeV. In addition to the standard configuration of physics objects in the analysis, an official SUSY PAT Cross cleaning tool is used to correct the energy balancing for events with overlapping objects.[1)].

The RA4-like cut-flow used in this analysis is the following:

- $N_{lepton} = 1$
- $N_{jets} \geq 3$, with $E_T^{j3} > 50$GeV
- $CaloMET_T > 100$GeV

The Monte Carlo (MC) data samples with the corresponding statistics, are listed in Table 2. The SM background processes are produced with the Madgraph MC generator, and include W+jets, $t\bar{t}$, as well as QCD N-jet events.

In table 3 the number of signal and background events is compared between the **optimal** SL isolation selection and the one recommended by the V + jets group for leptons with $P_T > 10$ GeV. Further results are also provided for leptons with $P_T > 5$GeV. In the final two rows the significance is reported for LM0 and LM1 respectively. The

[1)] An electron-jet cross-cleaning is applied if an isolated electron is found close to a jet within a cone of size 0.5, whereas the muon-jet cross-cleaning is applied only if a non-isolated muon is found close to a jet (within a cone of size 0.2).

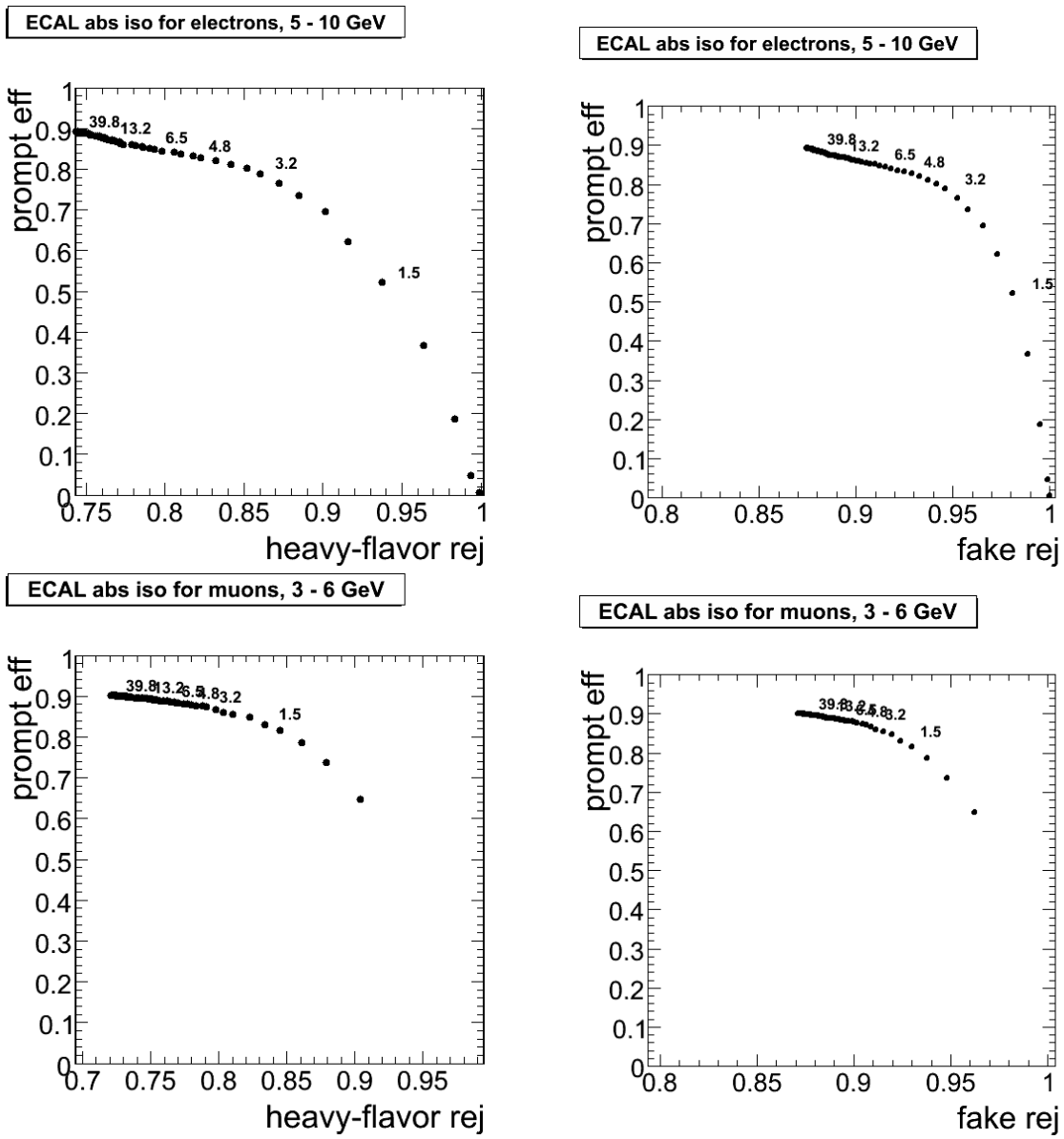

Figure 6: Prompt lepton efficiency with respect to HF (left) and fake (right) leptons rejection for different cuts on ECAL isolation. Top plots are for electrons in p_T range 5 – 10 GeV after a tracker isolation cut of 3 GeV. Bottom plots are for muons in p_T range 3 – 6 GeV after a tracker isolation cut of 5 GeV.

Sample	N MC events	σ (pb)
SUSY (LM0)	202686	110
SUSY (LM1)	104800	16.06
QCD, $250 < \hat{pT} < 500$ GeV	4874539	400000
QCD, $500 < \hat{pT} < 1000$ GeV	4570718	14000
QCD, $\hat{pT} > 1000$ GeV	1046863	370
$b\bar{b}$+jets, $250 < \hat{pT} < 500$ GeV	1052158	15000
$b\bar{b}$+jets, $500 < \hat{pT} < 1000$ GeV	985233	700
$b\bar{b}$+jets, $\hat{pT} > 1000$ GeV	327618	13
W+ jets	8900000	40000
$t\bar{t}$+jets	946644	317

Table 2: MC samples used in the SL analysis.

corresponding numbers when applying the **pureHF** cuts to muons and **pureFake** cu8ts to electrons are shown in table 4.

For both the electron and muon channels, the proposed **pure** and **optimal** SL isolation cuts produce a significant increase in the signal yield, since these cuts appear rather loose compared to the V+jets ones. The number of background events is increased as well, particularly from QCD processes. The **optimal** cuts show higher significance values than the **pure** for both muons and electrons.

In the electron channel, the significance increases while applying the SL isolation, despite the steep increase of QCD. The muon channel shows similarly an increase in the signal significance, mainly pronounced in the LM0 case. The move to a 5GeV lepton P_T threshold shows some improvement for muons, although this is minimal due to the reduced efficiency in the muon reconstruction (for muons below 10 GeV). In the electrons case, the significance reduces for LM0, and is barely improved for LM1. This indicates that switching to a threshold of 5GeV in the electron momentum may not be beneficial.

The above event yield comparison confirms that it is possible to improve the signal significance of the single lepton analysis whilst using low-P_T leptons. The soft lepton isolation performance shows comparable significance between the **optimal** and the **pure** selection. In the 1-muon channel, the attempt of lowering the muon momentum threshold to 5GeV P_T shows a profitable gain in the signal significance, whereas in the 1-electron, the maintenance of the 10 GeV threshold may be preferable.

Sample	e			μ		
	V+j$_{pt_{10}}$	SL$_{\mathbf{opt}:pt_{10}}$	SL$_{\mathbf{opt}:pt_5}$	V+j$_{pt_{10}}$	SL$_{\mathbf{opt}:pt_{10}}$	SL$_{\mathbf{opt}:pt_5}$
SUSY(LM0)	364.0	423.1	426.1	512.5	604.0	709.8
SUSY(LM1)	58.5	73.9	78.4	87.0	97.7	124.2
$t\bar{t}$	278.6	328.8	334.2	376.7	424.0	467.7
W+jets	159.7	192.1	198.7	182.2	206.5	229.0
QCD (250-500)	0.0	8.2	8.2	0.0	41.0	73.9
QCD (500-1000)	1.2	2.5	5.5	1.2	34.6	84.8
QCD (1000-inf)	0.5	0.9	1.3	0.1	2.5	8.8
$bb+$ jets (250-500)	0.0	0.0	0.0	1.4	15.7	37.1
$bb+$ jets (500-1000)	0.1	0.8	0.5	0.4	12.4	28.1
$bb+$ jets (1000-inf)	0.1	0.1	0.1	0.1	0.8	1.7
$S/\sqrt{S+B}$ (LM0)	17.3	18.3	18.2	21.6	22.2	23.2
$S/\sqrt{S+B}$ (LM1)	2.8	3.2	3.4	3.7	3.6	4.1

Table 3: Number of events in the single electron and muon final states, for 100pb^{-1} of integrated luminosity, for the V + jets and the proposed **optimal** soft lepton isolation (SL). The lepton p_T cut for the V + jets and SL$_{\mathbf{opt}:pt_{10}}$ is 10 GeV while $SL_{\mathbf{opt}:pt_5}$ is 5 Gev. In the last two rows the significance is reported for both LM0 and LM1

5.2 Same Sign DiLepton analysis

The SSDL analysis comprise a general-purpose search for supersymmetry in events containing two same sign leptons of any combination of flavors, in addition to multiple jets and large missing transverse energy. The require-

Sample	e			μ		
	V+j$_{pt_{10}}$	SL$_{\mathbf{pur}:pt_{10}}$	SL$_{\mathbf{pur}:pt_5}$	V+j$_{pt_{10}}$	SL$_{\mathbf{pur}:pt_{10}}$	SL$_{\mathbf{pur}:pt_5}$
SUSY(LM0)	364.0	417.8	418.2	512.5	584.2	665.09
SUSY(LM1)	58.5	73.5	77.6	87.0	95.8	120.4
$t\bar{t}$	278.6	325.0	327.8	376.7	418.2	456.5
W+jets	159.7	192.1	198.7	182.2	205.6	226.6
QCD (250-500)	0.0	8.2	8.2	0.0	24.6	41.0
QCD (500-1000)	1.2	2.5	5.2	1.2	23.6	50.5
QCD (1000-inf)	0.5	0.9	1.3	0.1	1.8	5.8
$b\bar{b}+$ jets (250-500)	0.0	0.0	0.0	1.4	11.4	25.7
$b\bar{b}+$ jets (500-1000)	0.1	0.5	0.8	0.4	8.6	18.7
$b\bar{b}+$ jets (1000-inf)	0.1	0.1	0.1	0.1	0.6	1.2
$S/\sqrt{S+B}$ (LM0)	17.3	18.2	18.	21.6	22.2	23.1
$S/\sqrt{S+B}$ (LM1)	2.8	3.2	3.3	3.7	3.6	4.2

Table 4: Number of events in the single electron and muon final states, for 100pb^{-1} of integrated luminosity, for the V + jets and the proposed **pure** soft lepton isolation (SL) (**pureHF** for muons, and **pureFake** for electrons). The lepton p_T cut for the V + jets and SL$_{\mathbf{pur}:pt_{10}}$ is 10 GeV while $SL_{\mathbf{pur}:pt_5}$ is 5 Gev. In the last two rows the significance is reported for both LM0 and LM1

ment of two same sign leptons significantly reduces the background contribution and provides very clear signature for discovery of SUSY at LHC.

The CMS SUSY group provides a set of baseline selection criteria for Single-lepton Reference Analysis 5 (RA5) [7]. A complete description of the SSDL analysis strategy and selection can be found elsewhere [8]. In addition to the standard configuration of physics objects in the analysis, we introduce the usage of the official SUSY PAT Cross cleaning tool.

To select events the following basic cuts were applied:

- MET trigger (MET $>$ 50 GeV)
- $HT =>$ 350 GeV
- $N_{lept} > 1$
- First and second lepton (classified in p_T) with same charge

The samples used for this study are reported in Tab. 5.

In table 6 the number of signal and background events expected at 10 TeV with 100 pb^{-1} with the proposed lepton selection is compared with the results of the recommended selection by the V + jets group (with $P_t > 10$ GeV). Final states with taus will not be considered for this comparison.

6 Summary

First CMS study of lepton isolation in p_T region below 30 GeV is presented to be used in SUSY analysis. Isolation variables based on tracking, ECAL and HCAL information separately as well as combined isolation were examined. The track-based isolation procedure demonstarated more efficient performance than other types of isolation, which makes it more attractive for the low-p_T regime, especially in the CMS start-up scenario. An additional rejection power of the isolation procedure can be achived by applying ECAL isolation cuts.

Four different isolation cuts optimization strategies are investigated and set of cut values and expected performances are provided. The proposed selections were applied to Single Lepton and Samie Sign Dilepton SUSY analyses. In both cases the improvement with respect to the standard V+jets prescription in the significance(15-30%) is observed. It is also demonstrated that with the proposed isolation the lepton momentum can be lowered from 10 to 5 GeV without lost in signal-to-background significance.

Sample	N MC events	σ (pb)
SUSY (LM0)	202686	110
SUSY (LM1)	104800	15.06
QCD $80 < \hat{pt} < 170$ GeV	3437680	1934640
QCD $170 < \hat{pt} < 300$ GeV	3746780	62563
QCD $300 < \hat{pt} < 470$ GeV	1810585	3665
QCD $470 < \hat{pt} < 800$ GeV	2406752	316
QCD $800 < \hat{pt} < 1400$ GeV	2907476	11.9
QCD $1400 < \hat{pt} < 2200$ GeV	584256	0.172
QCD $2200 < \hat{pt} < 3000$ GeV	878796	0.00142
QCD $\hat{pt} > 3000$ GeV	567040	0.0000086
W+ jets	8900000	40000
Z+jets	1262816	3700
$t\bar{t}$+jets	946644	317
WW	204722	44.8
ZZ	199810	17.4
WZ	246550	7.1
WW (same sign DPS)	1000	0.0216

Table 5: MonteCarlo samples analyzed for the search of the SSDL events.

Sample	ee			$\mu\mu$			$e\mu$		
	V+j$_{pt_{10}}$	SL$_{pt_{10}}$	SL$_{pt_5}$	V+j$_{pt_{10}}$	SL$_{pt_{10}}$	SL$_{pt_5}$	V+j$_{pt_{10}}$	SL$_{pt_{10}}$	SL$_{pt_5}$
SUSY(LM0)	2.44	4.23	4.67	9.99	16.28	28.87	10.47	16.99	22.95
SUSY(LM1)	0.52	1.10	1.30	2.15	3.03	5.46	2.84	3.94	5.61
$t\bar{t}$	0.07	0.20	0.33	0.13	1.88	7.20	0.23	1.58	3.75
W/Z + jets	0.00	0.00	0.00	0.00	0.00	0.00	0.00	0.00	0.45
diBosons	0.02	0.02	0.02	0.02	0.13	0.03	0.01	0.01	0.04
QCD	0.00	0.00	0.00	0.00	0.20	5.64	0.00	0.00	1.93
$S/\sqrt{S+B}$ (LM0)	1.5	2.0	2.1	3.1	3.8	4.4	3.2	3.9	4.3
$S/\sqrt{S+B}$ (LM1)	0.7	1.0	1.0	1.4	1.3	1.3	1.6	1.7	1.6

Table 6: Number of events in the final states ee, $\mu\mu$, $e\mu$, for the V + jets and the proposed soft lepton isolation (SL). The lepton p_T cut for the V + jets and SL$_{pt_{10}}$ is 10 GeV while SL$_{pt_5}$ is 5 Gev. In the last row the significance is reported.

References

[1] https://twiki.cern.ch/twiki/bin/view/CMS/VplusJets

[2] https://twiki.cern.ch/twiki/bin/view/CMS/SusyPatLayer1

[3] https://twiki.cern.ch/twiki/bin/view/CMS/SusyICFNtuple

[4] **CMS AN-2008/082***"A cut based method for electron identification in CMS"*

[5] **CMS AN-2008/098***"Muon Identification in CMS"*

[6] https://twiki.cern.ch/twiki/bin/view/CMS/SusyRA4SingleLeptonOrganization

[7] https://twiki.cern.ch/twiki/bin/view/CMS/SusyRA5SSDiLeptonOrganization

[8] Analysis note in preparation *"Search for Supersymmetry in the Same-Sign Dilepton Final States"*

A Efficiency and rejection tables

This appendix is meant to provide for each optimized cut, the efficiency for prompt leptons and the rejection for HF and fake leptons. Electrons and muons results are given in subsections A.1 and A.2 respectively.

A.1 Tracker Isolation for Electrons

Tables 7, 8, 9 and 10 describe the results for pure$_{HF}$, pure$_{fake}$, optimized and efficient optimization procedures.

p_T range (GeV)	Optimal cut	eff	rej$_{HF}$	rej$_{fake}$
5 - 10	1.83	0.872 ± 0.048	0.784 ± 0.0018	0.908 ± 0.00024
10 - 15	3.83	0.908 ± 0.042	0.825 ± 0.0021	0.904 ± 0.00032
15 - 20	4.5	0.918 ± 0.045	0.877 ± 0.0023	0.902 ± 0.00043
20 - 25	5.83	0.923 ± 0.05	0.888 ± 0.0027	0.904 ± 0.00053
25 - 30	6.5	0.932 ± 0.054	0.887 ± 0.0033	0.903 ± 0.0006

Table 7: Performances of the tracker isolation for electrons when the rejection of fakes is fixed at ≥ 0.9

p_T range (GeV)	Optimal cut	eff	rej$_{HF}$	rej$_{fake}$
5 - 10	-9.9	-9.9 $\pm$ -9.9	-9.9 $\pm$ -9.9	-9.9 $\pm$ -9.9
10 - 15	1.83	0.861 ± 0.051	0.903 ± 0.0016	0.94 ± 0.00026
15 - 20	3.5	0.905 ± 0.048	0.908 ± 0.002	0.919 ± 0.00039
20 - 25	5.17	0.918 ± 0.051	0.907 ± 0.0025	0.915 ± 0.0005
25 - 30	5.5	0.928 ± 0.056	0.906 ± 0.003	0.916 ± 0.00056

Table 8: Performances of the tracker isolation for electrons when the rejection of heavy flavor is fixed at ≥ 0.9

p_T range (GeV)	Optimal cut	eff	rej$_{HF}$	rej$_{fake}$
5 - 10	2.5	0.893 ± 0.044	0.76 ± 0.0019	0.889 ± 0.00027
10 - 15	3.5	0.905 ± 0.043	0.843 ± 0.002	0.911 ± 0.00031
15 - 20	3.83	0.912 ± 0.046	0.899 ± 0.0021	0.913 ± 0.00041
20 - 25	4.5	0.912 ± 0.053	0.913 ± 0.0024	0.924 ± 0.00047
25 - 30	4.17	0.915 ± 0.06	0.916 ± 0.0029	0.932 ± 0.00051

Table 9: Performances of the tracker isolation for electrons after minimizing the iso variable x

A.2 Tracker Isolation for Muons

Tables 11, 12, 13 and 14 describe the results for pure$_{HF}$, pure$_{fake}$, optimized and efficient optimization procedures.

p_T range (GeV)	Optimal cut	eff	rej$_{HF}$	rej$_{fake}$
5 - 10	3.17	0.903 ± 0.042	0.736 ± 0.0019	0.87 ± 0.00028
10 - 15	3.5	0.905 ± 0.043	0.843 ± 0.002	0.911 ± 0.00031
15 - 20	3.17	0.901 ± 0.049	0.925 ± 0.0018	0.924 ± 0.00038
20 - 25	3.83	0.903 ± 0.055	0.923 ± 0.0023	0.932 ± 0.00045
25 - 30	3.5	0.902 ± 0.064	0.924 ± 0.0027	0.937 ± 0.00049

Table 10: Performances of the tracker isolation for electrons when the prompt efficiency is fixed at ≥ 0.9

p_T range (GeV)	Optimal cut	eff	rej$_{HF}$	rej$_{fake}$
3 - 6	3.17	0.865 ± 0.06	0.775 ± 0.0011	0.903 ± 0.0004
6 - 9	11.8	0.938 ± 0.037	0.698 ± 0.0013	0.903 ± 0.00055
9 - 12	14.2	0.933 ± 0.043	0.738 ± 0.0015	0.901 ± 0.00082
12 - 15	16.8	0.952 ± 0.039	0.716 ± 0.0019	0.903 ± 0.0011
15 - 18	16.2	0.948 ± 0.044	0.755 ± 0.002	0.908 ± 0.0014
18 - 21	19.5	0.954 ± 0.046	0.728 ± 0.0023	0.9 ± 0.002
21 - 24	19.5	0.966 ± 0.043	0.723 ± 0.0028	0.906 ± 0.0023
24 - 27	22.2	0.962 ± 0.051	0.765 ± 0.0029	0.906 ± 0.0031
27 - 30	17.2	0.953 ± 0.062	0.788 ± 0.003	0.92 ± 0.0033

Table 11: Performances of the tracker isolation for muons when the rejection of fakes is fixed at ≥ 0.9

p_T range (GeV)	Optimal cut	eff	rej$_{HF}$	rej$_{fake}$
3 - 6	-9.9	-9.9 $\pm$ -9.9	-9.9 $\pm$ -9.9	-9.9 $\pm$ -9.9
6 - 9	1.83	0.835 ± 0.058	0.9 ± 0.00087	0.981 ± 0.00025
9 - 12	4.17	0.887 ± 0.054	0.902 ± 0.001	0.981 ± 0.00038
12 - 15	5.17	0.913 ± 0.052	0.903 ± 0.0012	0.977 ± 0.00058
15 - 18	6.17	0.914 ± 0.055	0.903 ± 0.0014	0.974 ± 0.0008
18 - 21	8.17	0.929 ± 0.057	0.901 ± 0.0016	0.964 ± 0.0013
21 - 24	8.5	0.949 ± 0.052	0.9 ± 0.0019	0.97 ± 0.0014
24 - 27	10.8	0.938 ± 0.063	0.903 ± 0.002	0.955 ± 0.0022
27 - 30	8.17	0.928 ± 0.075	0.901 ± 0.0022	0.977 ± 0.0018

Table 12: Performances of the tracker isolation for muons when the rejection of heavy flavor is fixed at ≥ 0.9

p_T range (GeV)	Optimal cut	eff	rej$_{HF}$	rej$_{fake}$
3 - 6	4.17	0.885 ± 0.056	0.748 ± 0.0011	0.886 ± 0.00043
6 - 9	6.83	0.918 ± 0.043	0.797 ± 0.0012	0.945 ± 0.00042
9 - 12	8.5	0.919 ± 0.046	0.833 ± 0.0013	0.951 ± 0.00059
12 - 15	8.83	0.934 ± 0.046	0.838 ± 0.0015	0.962 ± 0.00074
15 - 18	9.5	0.929 ± 0.051	0.857 ± 0.0016	0.959 ± 0.00099
18 - 21	9.17	0.934 ± 0.055	0.891 ± 0.0016	0.961 ± 0.0013
21 - 24	8.83	0.95 ± 0.052	0.9 ± 0.0019	0.969 ± 0.0014
24 - 27	15.2	0.948 ± 0.059	0.854 ± 0.0024	0.949 ± 0.0023
27 - 30	11.2	0.939 ± 0.07	0.866 ± 0.0025	0.96 ± 0.0024

Table 13: Performances of the tracker isolation for muons after minimizing the iso variable x

p_T range (GeV)	Optimal cut	eff	rej$_{HF}$	rej$_{fake}$
3 - 6	5.5	0.902 ± 0.053	0.716 ± 0.0012	0.867 ± 0.00046
6 - 9	4.5	0.901 ± 0.046	0.847 ± 0.0011	0.961 ± 0.00036
9 - 12	5.5	0.902 ± 0.051	0.878 ± 0.0011	0.976 ± 0.00042
12 - 15	4.17	0.902 ± 0.055	0.918 ± 0.0011	0.982 ± 0.00051
15 - 18	4.5	0.902 ± 0.059	0.931 ± 0.0012	0.979 ± 0.00072
18 - 21	4.5	0.906 ± 0.065	0.938 ± 0.0013	0.989 ± 0.00069
21 - 24	3.17	0.907 ± 0.069	0.958 ± 0.0013	0.99 ± 0.00079
24 - 27	5.83	0.902 ± 0.078	0.959 ± 0.0014	0.965 ± 0.0019
27 - 30	3.83	0.904 ± 0.086	0.959 ± 0.0015	0.988 ± 0.0013

Table 14: Performances of the tracker isolation for muons when the prompt efficiency is fixed at ≥ 0.9

B Efficiency and rejection plots for tracker isolation

In this appendix efficiency and background rejection plots are shown. The cut values to determine the curves are superimposed to the plots.

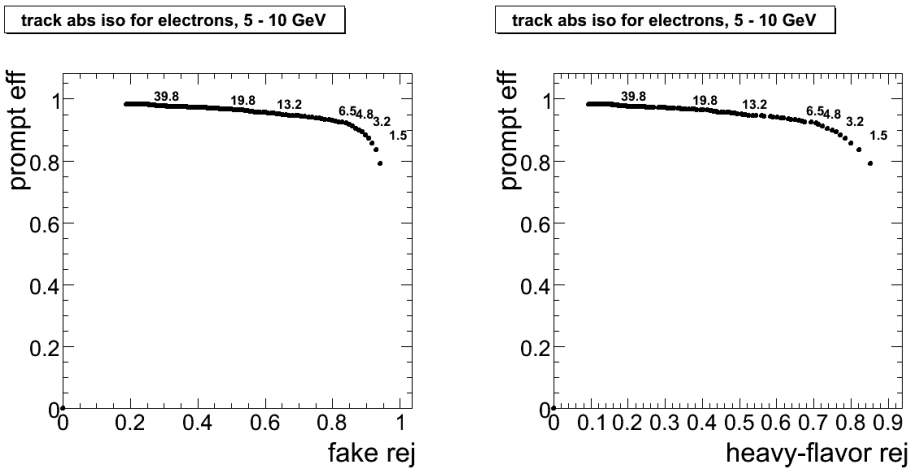

Figure 7: Prompt leptons efficiency with respect to background rejection for fake (left) and HF leptons (right) in pT region from 5 to 10 GeV for electrons. Cut values are superimposed to the curve.

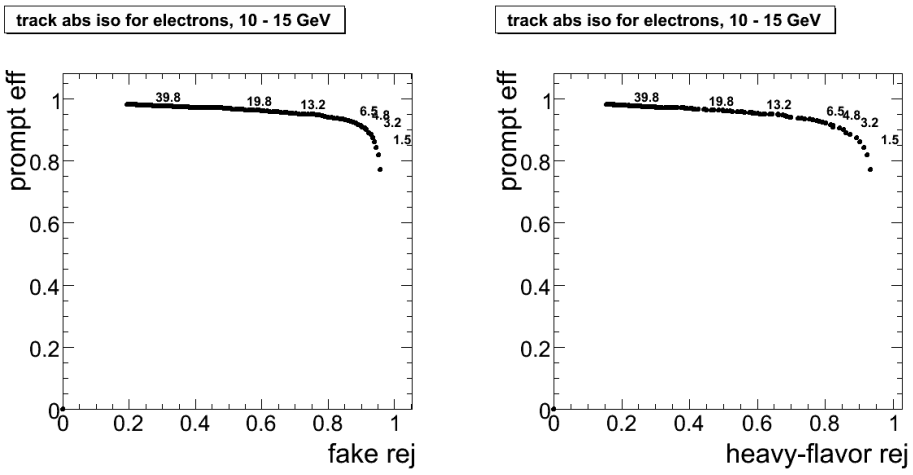

Figure 8: Prompt leptons efficiency with respect to background rejection for fake (left) and HF leptons (right) in pT region from 10 to 15 GeV for electrons. Cut values are superimposed to the curve.

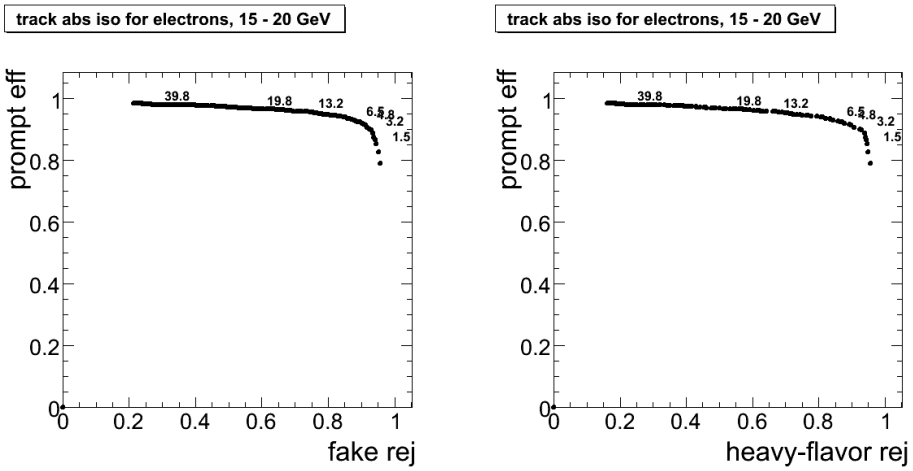

Figure 9: Prompt leptons efficiency with respect to background rejection for fake (left) and HF leptons (right) in pT region from 15 to 20 GeV for electrons. Cut values are superimposed to the curve.

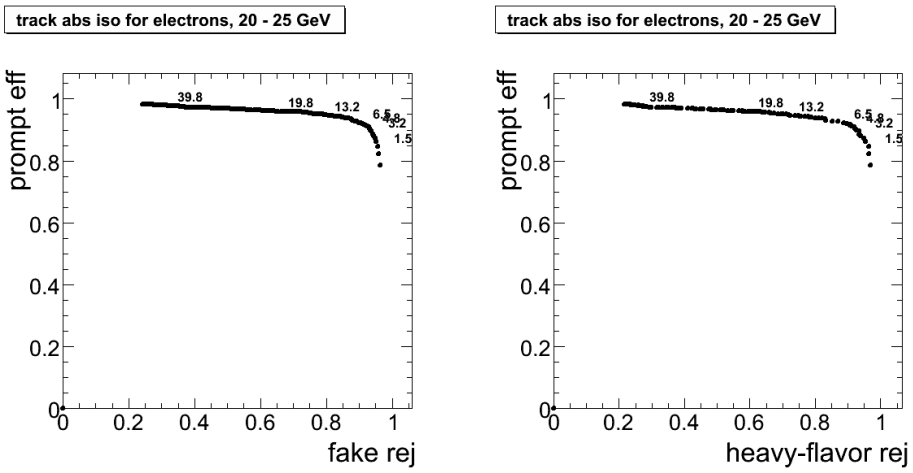

Figure 10: Prompt leptons efficiency with respect to background rejection for fake (left) and HF leptons (right) in pT region from 20 to 25 GeV for electrons. Cut values are superimposed to the curve.

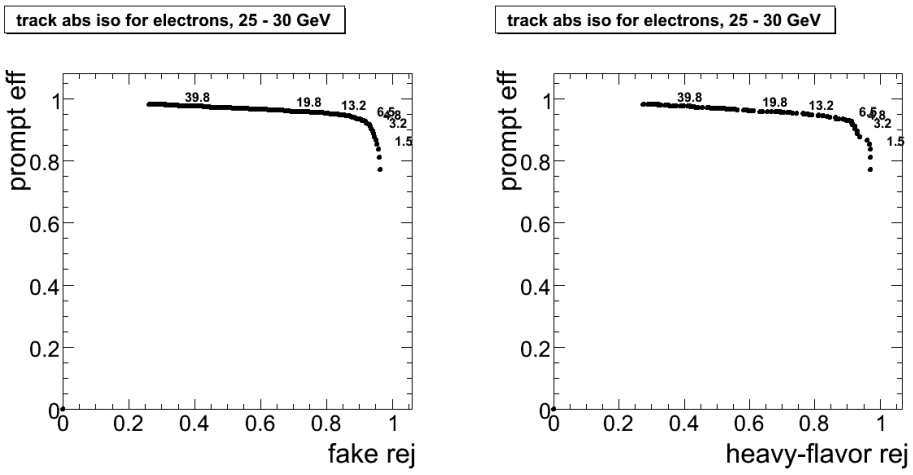

Figure 11: Prompt leptons efficiency with respect to background rejection for fake (left) and HF leptons (right) in pT region from 25 to 30 GeV for electrons. Cut values are superimposed to the curve.

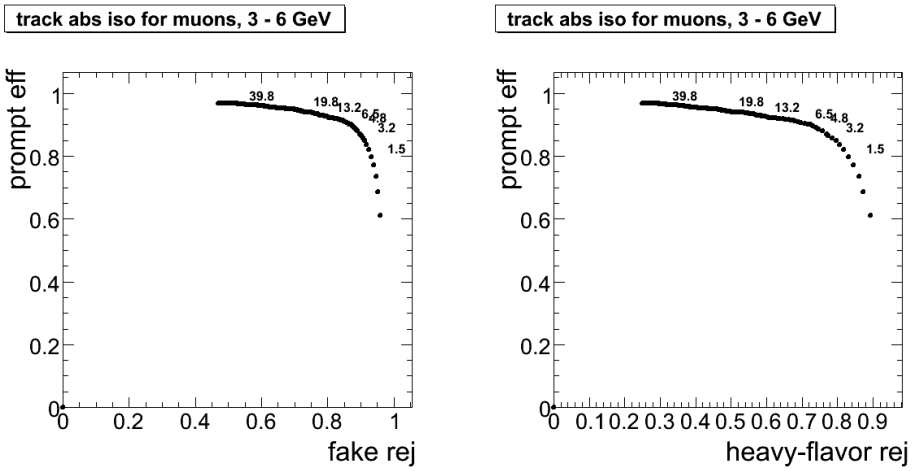

Figure 12: Prompt leptons efficiency with respect to background rejection for fake (left) and HF leptons (right) in pT region from 3 to 6 GeV for muons. Cut values are superimposed to the curve.

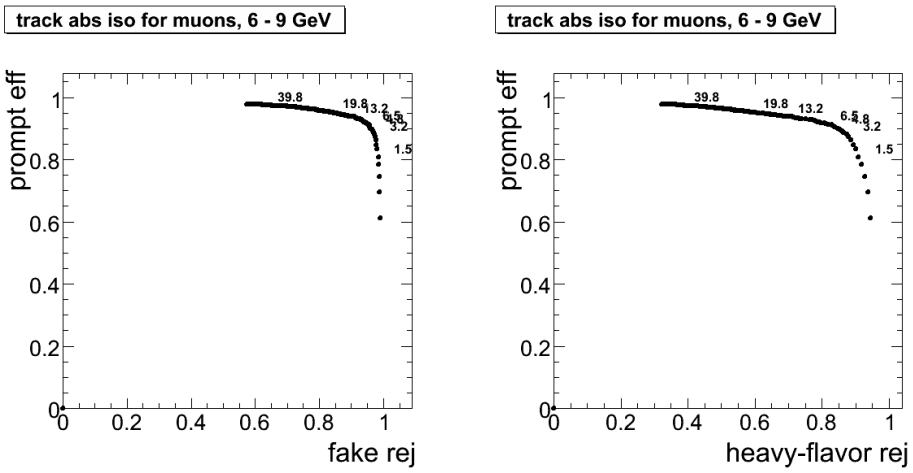

Figure 13: Prompt leptons efficiency with respect to background rejection for fake (left) and HF leptons (right) in pT region from 6 to 9 GeV for muons. Cut values are superimposed to the curve.

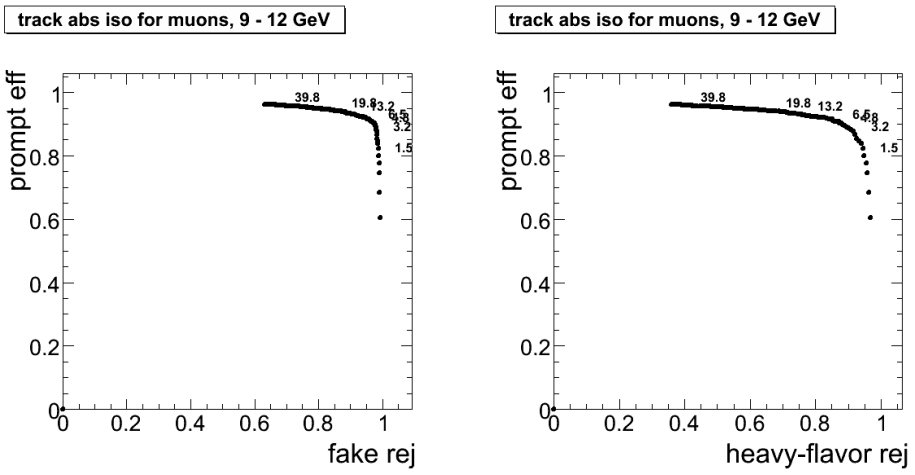

Figure 14: Prompt leptons efficiency with respect to background rejection for fake (left) and HF leptons (right) in pT region from 9 to 12 GeV for muons. Cut values are superimposed to the curve.

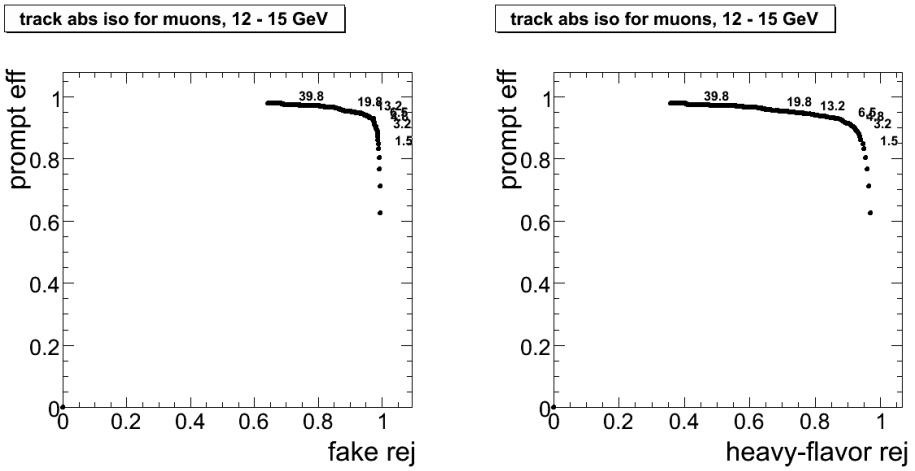

Figure 15: Prompt leptons efficiency with respect to background rejection for fake (left) and HF leptons (right) in pT region from 12 to 15 GeV for muons. Cut values are superimposed to the curve.

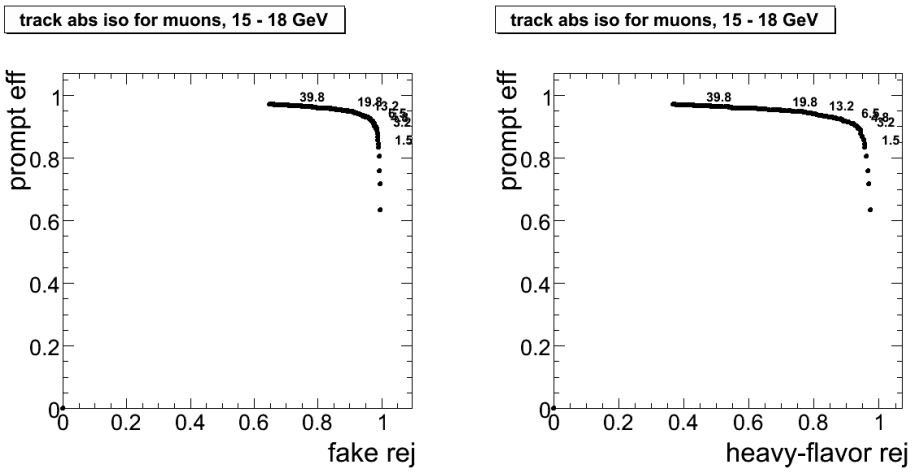

Figure 16: Prompt leptons efficiency with respect to background rejection for fake (left) and HF leptons (right) in pT region from 15 to 18 GeV for muons. Cut values are superimposed to the curve.

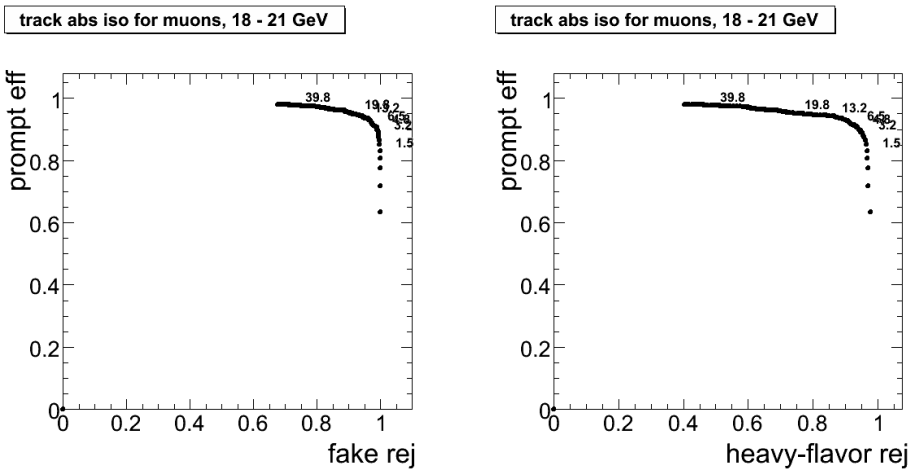

Figure 17: Prompt leptons efficiency with respect to background rejection for fake (left) and HF leptons (right) in pT region from 18 to 21 GeV for muons. Cut values are superimposed to the curve.

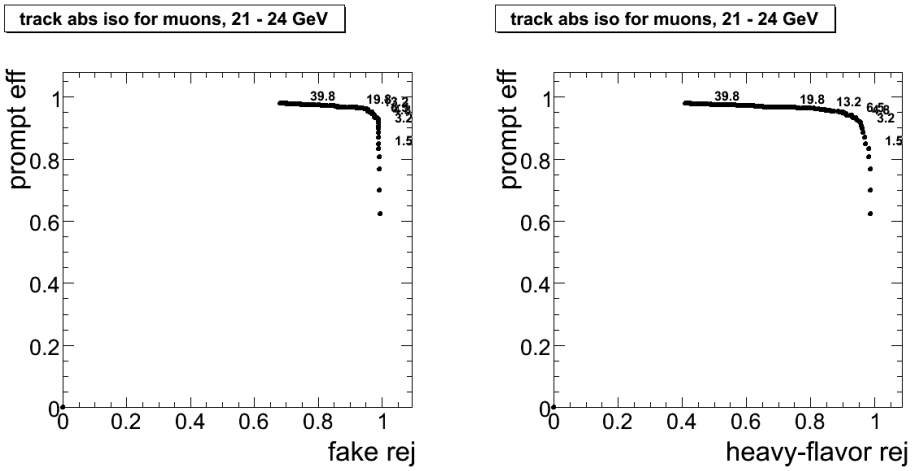

Figure 18: Prompt leptons efficiency with respect to background rejection for fake (left) and HF leptons (right) in pT region from 21 to 24 GeV for muons. Cut values are superimposed to the curve.

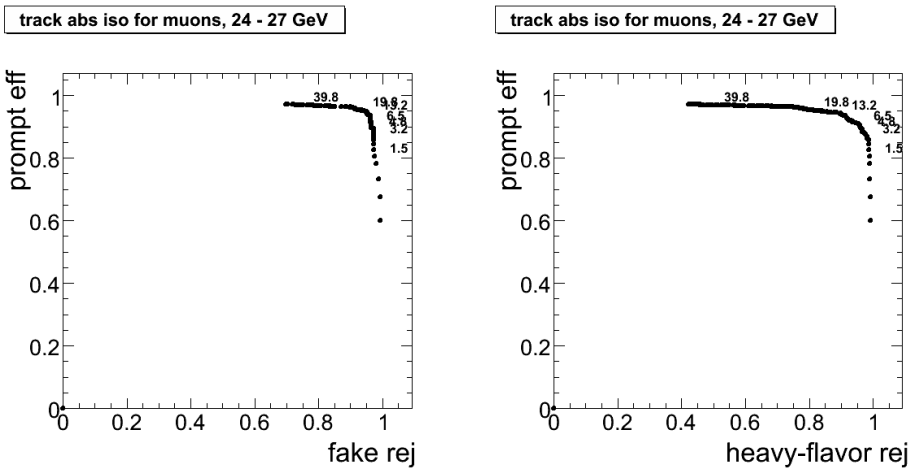

Figure 19: Prompt leptons efficiency with respect to background rejection for fake (left) and HF leptons (right) in pT region from 24 to 27 GeV for muons. Cut values are superimposed to the curve.

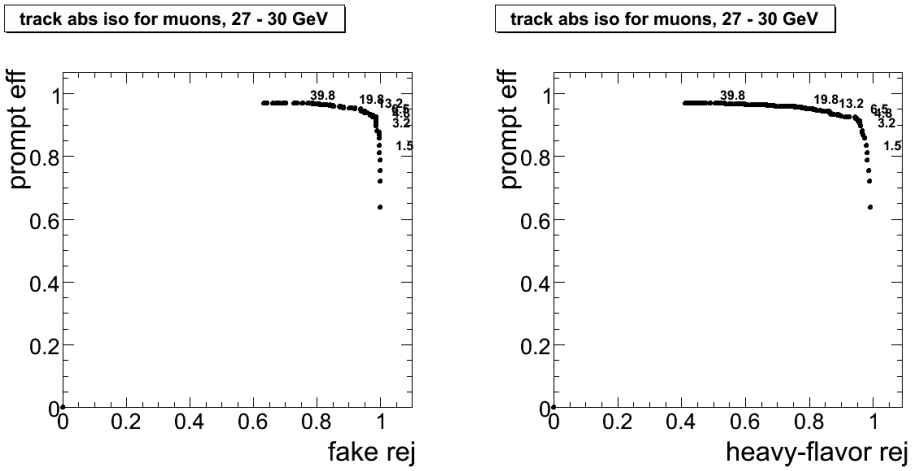

Figure 20: Prompt leptons efficiency with respect to background rejection for fake (left) and HF leptons (right) in pT region from 27 to 30 GeV for muons. Cut values are superimposed to the curve.

C Efficiency and rejection plots for ECAL isolation

In this appendix the efficiency versus rejection plots are shown for ECAL isolation. Efficiency is defined as the number of leptons which pass the tracker and ECAL isolation divide by the number of reconstructed leptons

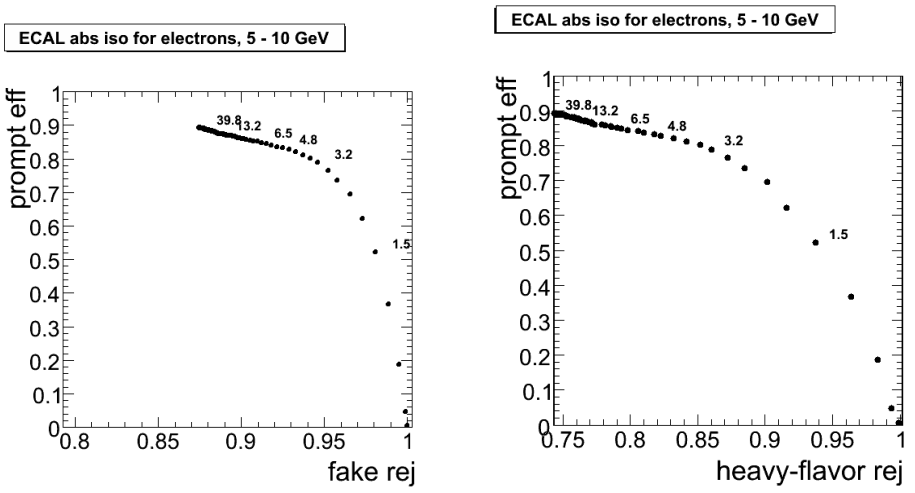

Figure 21: Prompt leptons efficiency with respect to background rejection for fake (left) and HF leptons (right) in pT region from 5 to 10 GeV for electrons. Cut values are superimposed to the curve.

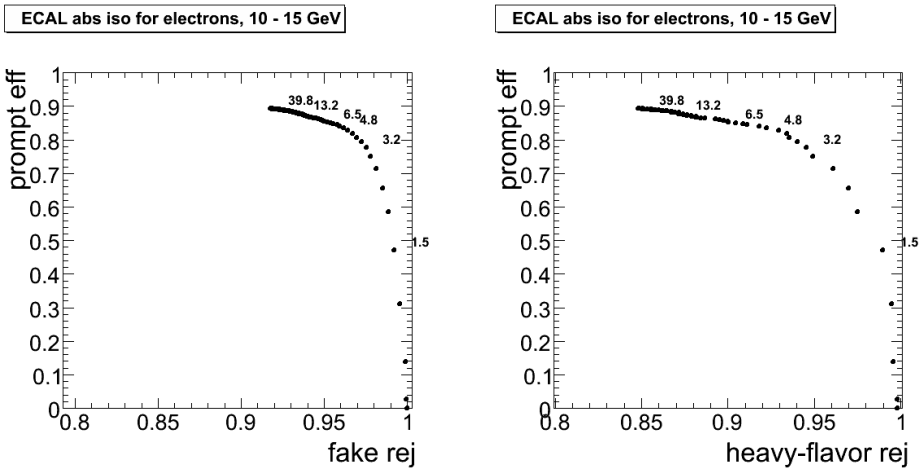

Figure 22: Prompt leptons efficiency with respect to background rejection for fake (left) and HF leptons (right) in pT region from 10 to 15 GeV for electrons. Cut values are superimposed to the curve.

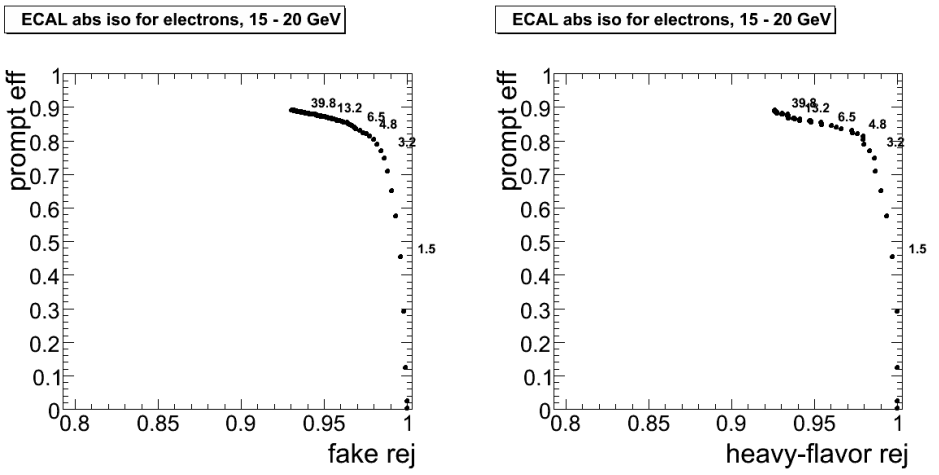

Figure 23: Prompt leptons efficiency with respect to background rejection for fake (left) and HF leptons (right) in pT region from 15 to 20 GeV for electrons. Cut values are superimposed to the curve.

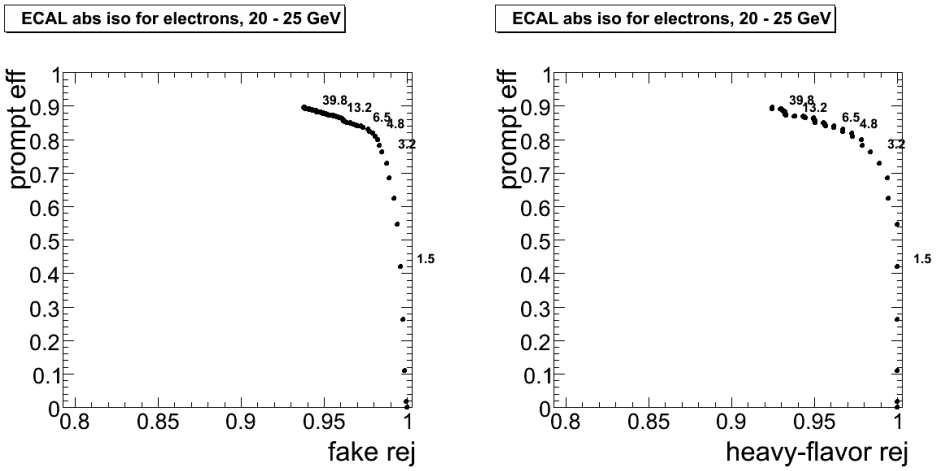

Figure 24: Prompt leptons efficiency with respect to background rejection for fake (left) and HF leptons (right) in pT region from 20 to 25 GeV for electrons. Cut values are superimposed to the curve.

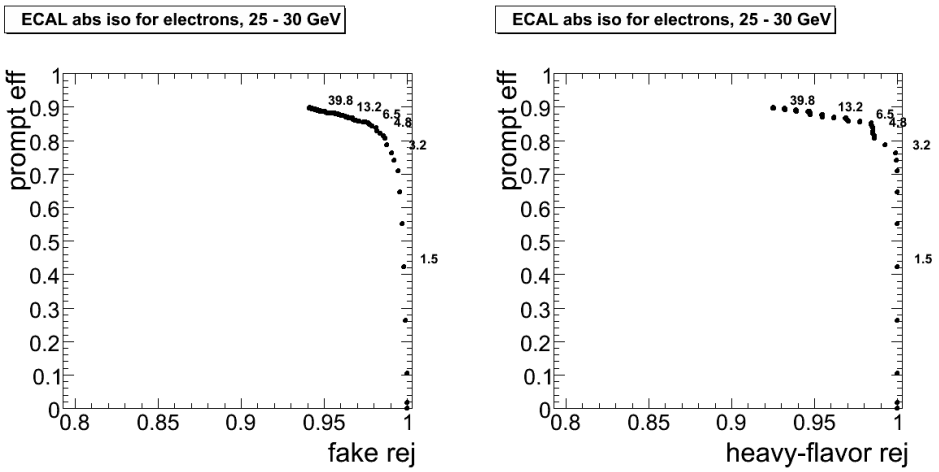

Figure 25: Prompt leptons efficiency with respect to background rejection for fake (left) and HF leptons (right) in pT region from 25 to 30 GeV for electrons. Cut values are superimposed to the curve.

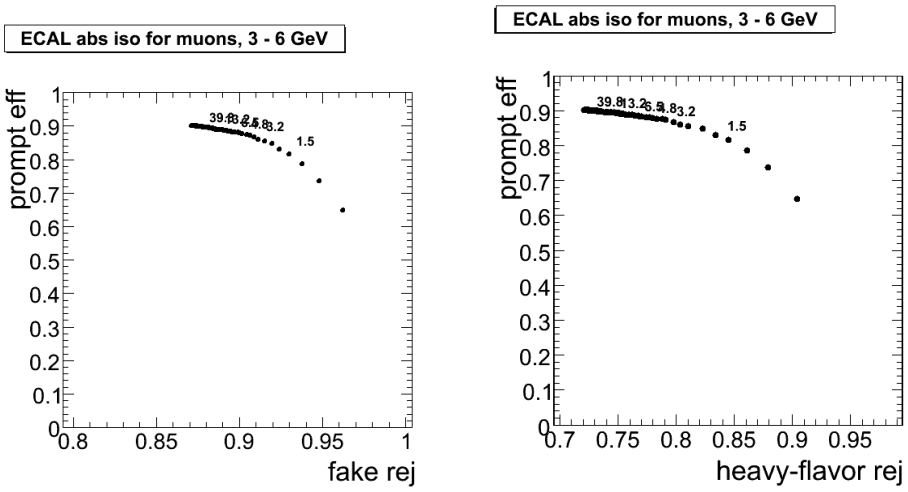

Figure 26: Prompt leptons efficiency with respect to background rejection for fake (left) and HF leptons (right) in pT region from 3 to 6 GeV for muons. Cut values are superimposed to the curve.

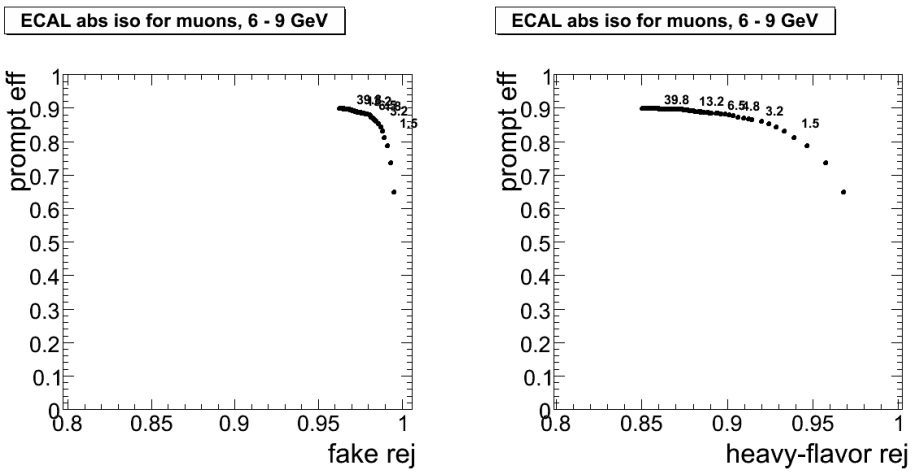

Figure 27: Prompt leptons efficiency with respect to background rejection for fake (left) and HF leptons (right) in pT region from 6 to 9 GeV for muons. Cut values are superimposed to the curve.

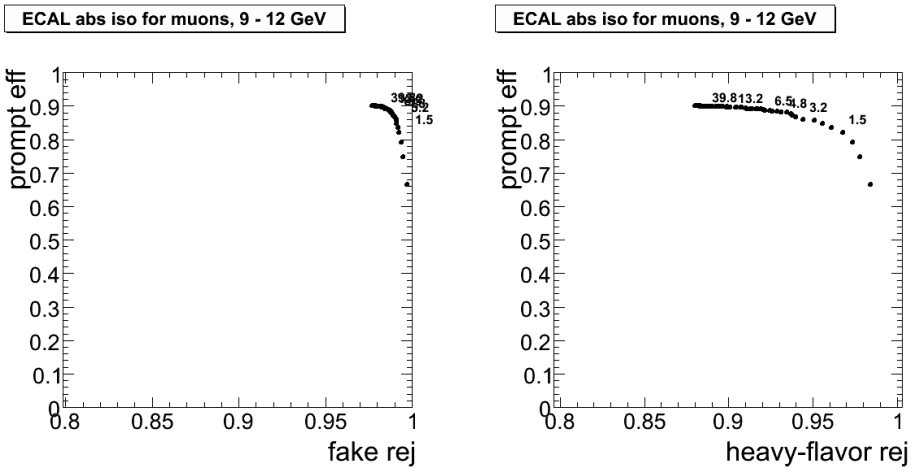

Figure 28: Prompt leptons efficiency with respect to background rejection for fake (left) and HF leptons (right) in pT region from 9 to 12 GeV for muons. Cut values are superimposed to the curve.

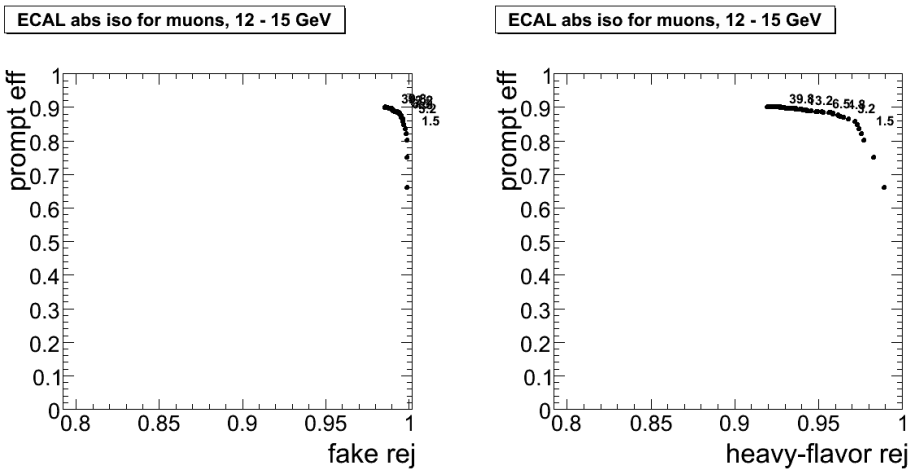

Figure 29: Prompt leptons efficiency with respect to background rejection for fake (left) and HF leptons (right) in pT region from 12 to 15 GeV for muons. Cut values are superimposed to the curve.

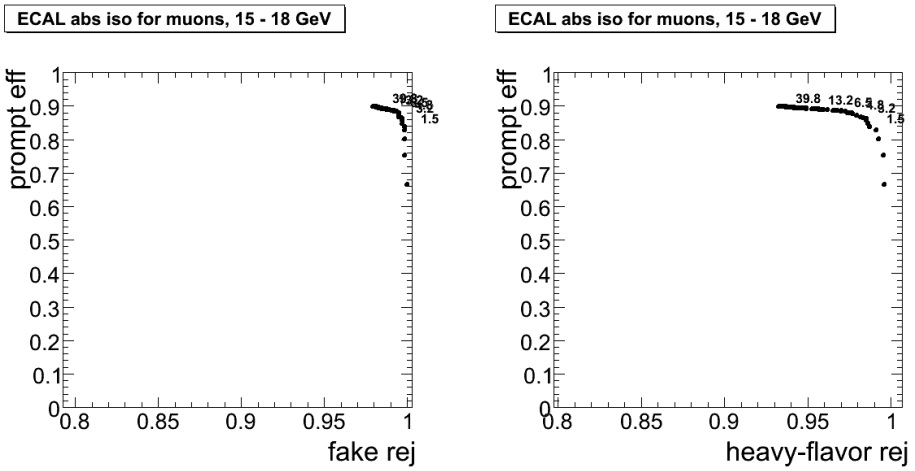

Figure 30: Prompt leptons efficiency with respect to background rejection for fake (left) and HF leptons (right) in pT region from 15 to 18 GeV for muons. Cut values are superimposed to the curve.

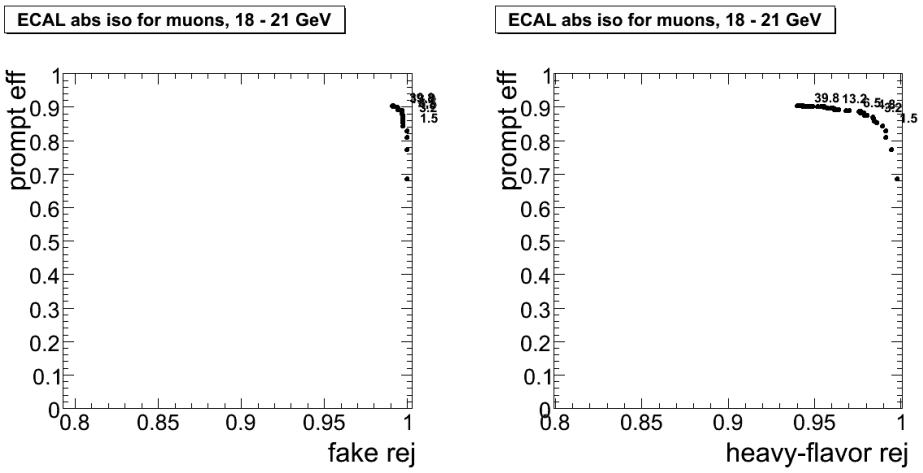

Figure 31: Prompt leptons efficiency with respect to background rejection for fake (left) and HF leptons (right) in pT region from 18 to 21 GeV for muons. Cut values are superimposed to the curve.

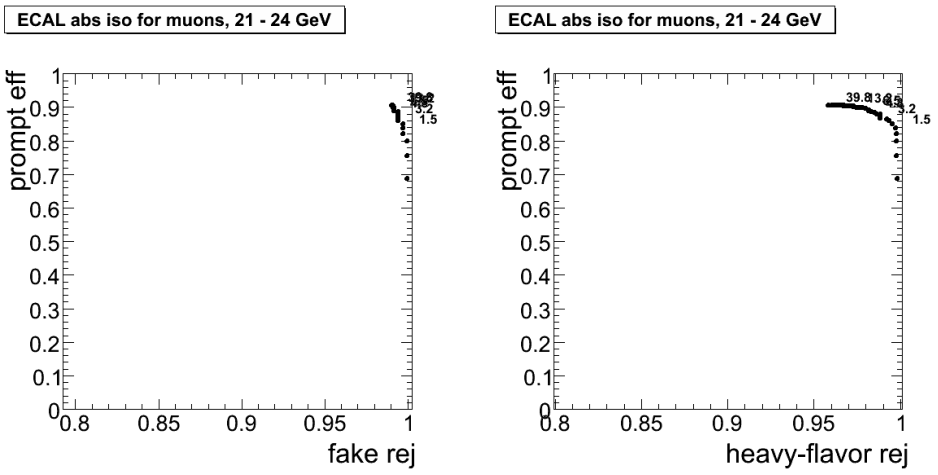

Figure 32: Prompt leptons efficiency with respect to background rejection for fake (left) and HF leptons (right) in pT region from 21 to 24 GeV for muons. Cut values are superimposed to the curve.

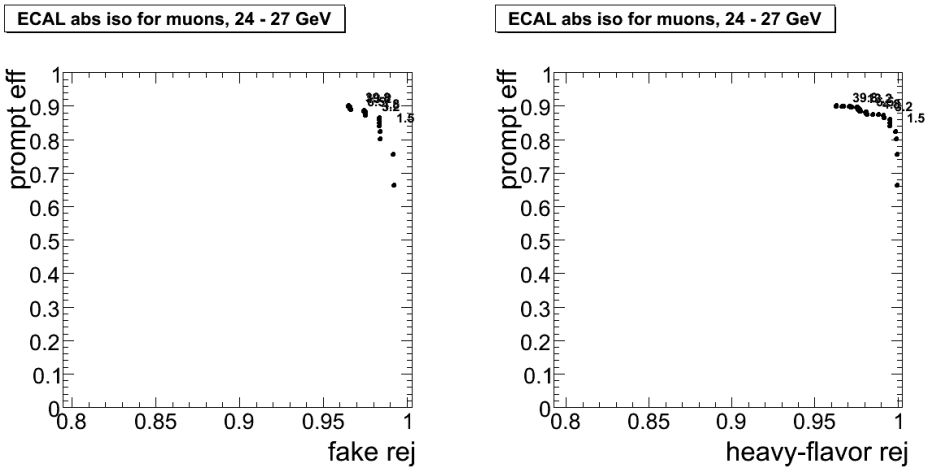

Figure 33: Prompt leptons efficiency with respect to background rejection for fake (left) and HF leptons (right) in pT region from 24 to 27 GeV for muons. Cut values are superimposed to the curve.

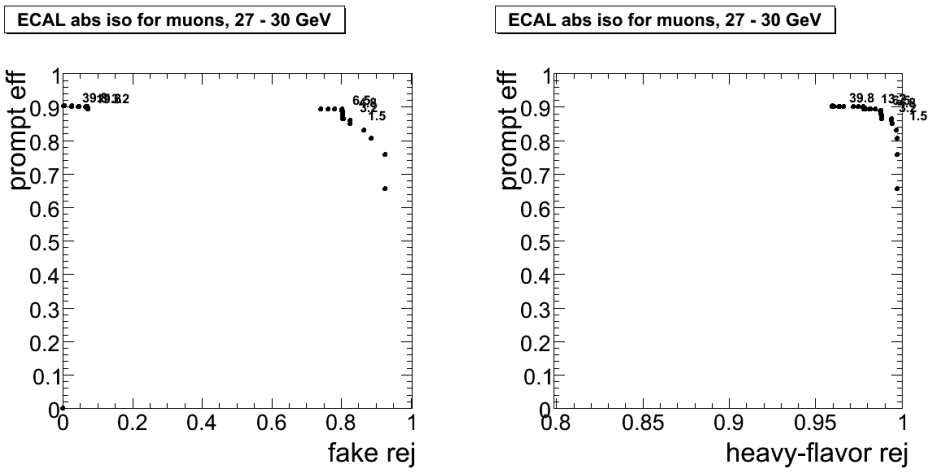

Figure 34: Prompt leptons efficiency with respect to background rejection for fake (left) and HF leptons (right) in pT region from 27 to 30 GeV for muons. Cut values are superimposed to the curve.

D The strange case of isolated muons

It has been observed that there is a sharp peak at zero in the isolation distributions both for fake muons and those coming heavy flavour decays. Since this is a surprising result and could reduce the effectiveness of an isolation cut in supressing the QCD background, it was important to understand the causes of this effect. In order to do this, a generator level study was undertaken.

For a reconstructed muon, we may calculate a generator level tracker isolation quantity GenIso. This is defined as follows:

$$\text{GenIso} = \sum_{0.01<\Delta R<0.3} p_{\text{T}}^{\text{GEN}} \tag{1}$$

where the sum is taken over generator level particles with $p_T > 200$ MeV (this matches the threshold in offline track reconstruction). Figure **??** shows a comparison of GenIso and absolute tracker isolation for muons coming from heavy flavour decays. It can be seen that GenIso shows very similar behaviour to the tracker isolation and thus the zero peak is a genuine effect.

By investigating the origins of the generator level muon and the particles contributing to the isolation, it was found that two effects contribute towards the peak. Firstly, in a small number of cases, jet fragmentation will lead to zero charged particles emerging from the decay of the b quark. In this case, even if the muon is colinear with the jet, the tracker isolation will be zero (this does not explain the fact that zero peaks are also seen in the ECAL and HCAL isolations). The second effect is from asymmetric b decays where either the muon or associated D meson takes a larger share of the p_T of the B meson. This can cause the muon to be separated from the jet and also lead to zero isolation. In many cases, these effects will combine accounting for the $\sim 3\%$ of events seen in the zero isolation peak.